Bioorganic Chemistry 86 (2019) 187–196

Contents lists available at ScienceDirect

Bioorganic Chemistry

journal homepage: www.elsevier.com/locate/bioorg

Mono- or di-substituted imidazole derivatives for inhibition of acetylcholine and butyrylcholine esterases

Burak Kuzu[a,b], Meltem Tan[a,b], Parham Taslimi[c], İlhami Gülçin[c], Mehmet Taşpınar[d], Nurettin Menges[a,b,*]

[a] Pharmaceutical Chemistry Section, Van Yuzuncu Yil University, 65080 Van, Turkey
[b] SAFF Chemical Reagent R&D Lab. YYU-TEKNOKENT, 65080 Van, Turkey
[c] Department of Chemistry, Atatürk University, 25240 Erzurum, Turkey
[d] Department of Medicinal Biology, Van Yuzuncu Yil University, 65080 Van, Turkey

ARTICLE INFO

Keywords:
SAR
Docking
Alzheimer's disease
Water solubility
ADME
Enzyme kinetic study

ABSTRACT

Mono- or di-substituted imidazole derivatives were synthesized using a one-pot, two-step strategy. All imidazole derivatives were tested for AChE and BChE inhibition and showed nanomolar activity similar to that of the test compound donepezil and higher than that of tacrine. Structure activity relationship studies, docking studies to on X-ray crystal structure of AChE with PDB code 1B41, and adsorption, distribution, metabolism, and excretion (ADME) predictions were performed. The synthesized core skeleton was bound to important regions of the active site of AChE such as the peripheral anionic site (PAS), oxyanion hole (OH), and anionic subsite (AS). Selectivity of the reported test compounds was calculated and enzyme kinetic studies revealed that they behave as competitive inhibitors, while two of the test compounds showed noncompetitive inhibitory behavior. ADME predictions revealed that the synthesized molecules might pass through the blood brain barrier and intestinal epithelial barrier and circulate freely in the blood stream without binding to human serum albumin. While the toxicity of one compound on the WS1 (skin fibroblast) cell line was 1790 μM, its toxicity on the SH-SY5Y (neuroblastoma) cell line was 950 μM.

1. Introduction

Alzheimer's disease (AD) is one of the most important disorders and is irreversible. It is a progressive brain disorder that slowly destroys memory, thinking skills, and the ability to carry out simple tasks [1,2]. Altered levels of acetylcholine (ACh) in hippocampal and cortical regions lead to cholinergic system dysfunction, resulting in severe memory and learning deficits. One therapeutic approach to enhance cholinergic neurotransmission is to increase ACh availability by inhibiting acetylcholinesterase (AChE) [3–7]. Thus far, several anti-AD drugs targeting ChEs have become available, including tacrine [8], donepezil [9], rivastigmine [10], and the alkaloid galantamine [11] (see Fig. 1).

However, no drugs have significantly affected the symptoms or stopped the progression of the disease in clinical studies. Many research groups are studying AChE inhibitors, as the level of ACh is crucial for AD therapy. Indole-containing piperidine derivatives [12], tacrine-based and carbamate derivatives [13], selenium-piperidine derivatives [14], *p*-aminobenzoic acid derivatives [15], and coumarin-type carbamate derivatives [16] were tested for AChE inhibition. In addition, Moon et al. researched oxotremorine derivatives, which possess imidazole, pyrrole, and triazole rings, and achieved nanomolar activity using N,N-di-imidazole propargyl amine derivatives [17a]. There are many studies in progress on AD in which structural motifs such as piperidine, alkyl chain spacer, carbamate, and methoxy groups serve as active pharmacophore groups. Gurjar et al. have found out that imidazole derivatives showed good potencies on inhibition of ChEs [17b]. These studies prompted us to search C-2 and C-4 substituted or C-2 substituted imidazole derivatives for inhibition of AChE and BChE.

Abbreviations: AChE, acetylcholinesterase; BChE, butyrylcholinesterase; ACh, acetylcholine; AD, Alzheimer's disease; BBB, blood-brain barrier; CAS, catalytic site; ES, acetyl ester; PAS, peripheral anionic site; Log P, lipophilicity; Log_{KHSA}, human serum albumin binding; WS1, skin fibroblast cell line; SH-SY5Y, neuroblastoma cell line; ADME, adsorption distribution metabolism excretion

* Corresponding author at: Pharmaceutical Chemistry Section, Van Yuzuncu Yil University, 65080 Van, Turkey.
E-mail address: nurettinmenges@yyu.edu.tr (N. Menges).

https://doi.org/10.1016/j.bioorg.2019.01.044
Received 26 October 2018; Received in revised form 18 January 2019; Accepted 19 January 2019
Available online 24 January 2019
0045-2068/

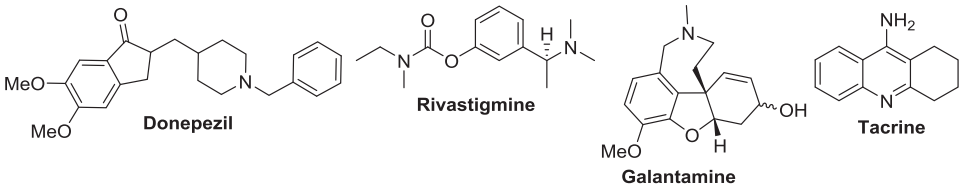

Fig. 1. Clinically used drugs for inhibition of ChEs.

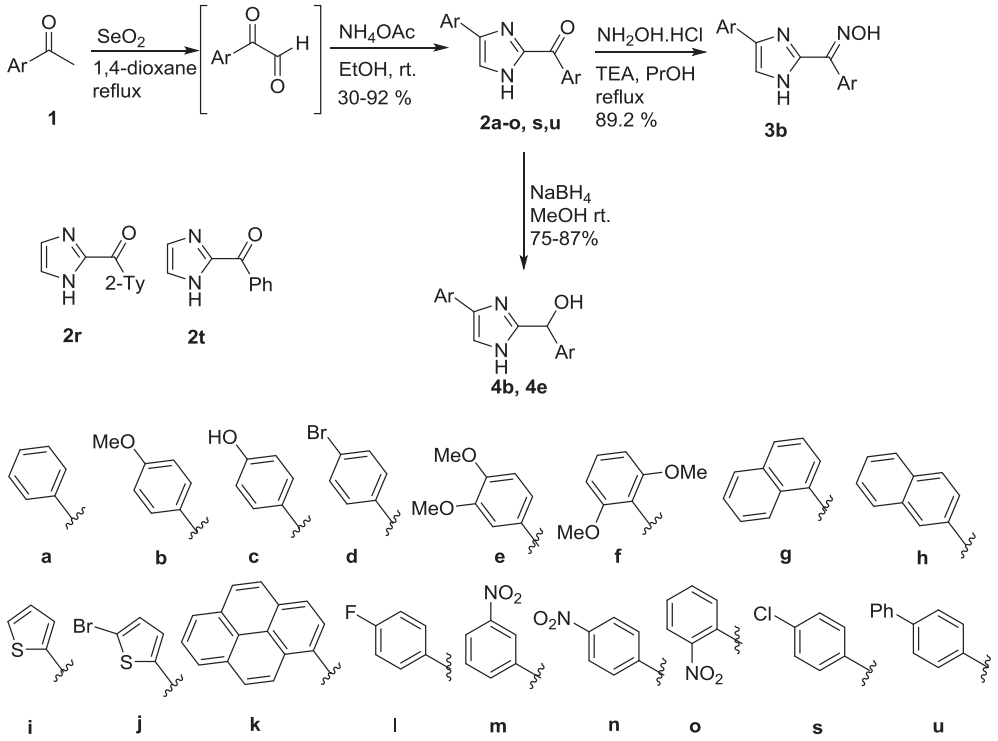

Scheme 1. Synthesis of imidazole derivatives (synthetic strategy for 2r and 2t is explained in SI).

2. Results and discussion

2.1. Synthesis

We synthesized imidazole derivatives **2a–o**, **2s**, and **2u** using a one-pot, two-step procedure based on our previous study (Scheme 1) [18]. To extend the study and the modulate structure–activity relationship (SAR), the condensation reaction was performed *via* a reaction between compound **2b** and hydroxyl amine in propanol at reflux temperature, giving rise to product **3b**. Compounds **2b** and **2e** were reduced by $NaBH_4$ to obtain **4b** and **4e**, which are racemic.

2.2. Cholinesterase activity and structure-activity relationship (SAR) study

Imidazole molecules have similar cores with an aroyl group at the C-2 position and an aryl group at the C-4 position. IC_{50} values of BChE were between 27.02 and 151.2 nM, whereas those of AChE were between 17.3 and 120.9 nM. While the clinically used reference drug tacrine displayed inhibition at 698.6 nM [19], donepezil displayed inhibition at 32.9 nM [20]. Thus, the reported imidazole molecules showed approximately 40- and 20-fold higher activity than tacrine and similar or higher activity than donepezil (Table 1).

For the SAR model, we chose compound **2a**, which has benzoyl and phenyl groups, and showed inhibition at 34.65 nM for AChE and at 61.27 nM for BChE. Compound **2b,** which has one methoxy group at the para-position of the phenyl ring, did not change the inhibition constant for AChE and revealed less activity on BChE than that of **2a**. Two methoxy groups at the *meta*- and para-positions of the phenyl ring (compound **2e**) increased the inhibition ability from 34.65 nM to 17.33 nM for AChE and from 61.27 nM to 41.67 nM for BChE. The clinically used molecule donepezil possesses the same sub-structure. SAR studies for donepezil show that two vicinal methoxy groups and a short linker increased biological activity up to 25-fold [21,22]. Replacement of methoxy groups with hydroxyl groups at the same position did not change the AChE activity but increased BChE activity. We tested the positional effect of the di-methoxy groups, and placement at both ortho-positions (compound **2f**) induced good inhibition, as seen in compound **2e**. The conversion of the phenyl ring to α-naphthyl, β-naphthyl, or pyrene was also evaluated. Compound **2g**, which has α-naphthyl groups, showed good inhibition for AChE and BChE. We hypothesized that more than one phenyl ring would increase the inhibition due to a better fit in the active site of the enzyme through π-π interactions due to the aromatic gorge of ChEs. We tested compound **2h,** which has Ar = β-naphthyl, to assess the effect of the position of the naphthyl group on inhibition activity. Surprisingly, we observed that the position of the naphthyl ring is important for a correct match, which was confirmed by Linusson et al. [23]. To understand the importance of the position of the phenyl ring with one more example, para-biphenyl derivative (**2u**) sharply decreased inhibition activity in which BChE was inhibited with the worst concentration (151.2 nM) within imidazole derivatives. The pyrene-substituted imidazole derivative **2k** exhibited potent AChE and BChE inhibitory activities with IC_{50} values of 17.32 and 64.28 nM, respectively, seen in compound **2g**. A similar result was reported in the literature in which caproctamine was modified by placing a pyrene-type bulky aromatic molecule, benzophenanthridine, causing nanomolar inhibitor activity due to π-π

Table 1
Human Acetylcholinesterase and Butyrylcholinesterase (AChE, BChE) inhibition and some predicted values.

Entry	IC_{50} (nM) AChE	IC_{50} (nM) BChE	K_i (nM) AChE	K_i (nM) BChE	AChE/ BChE	Log BB[a]	Log K_{HSA}[b]	Log P	Caco-2 Permeability[c]
2a	34.7 ± 1.56	61.27 ± 2.07	4.49 ± 1.65	30.08 ± 5.98	0.149	−0.366	0.299	3.396	1598
2b	34.7 ± 2.83	70.16 ± 0.65	4.31 ± 0.99	43.01 ± 12.11	0.100	−0.979	0.359	3.159	673
2c	34.6 ± 3.50	49.04 ± 1.83	14.32 ± 7.00	33.83 ± 7.76	0.423	−1.466	−0.137	1.624	163
2d	23.0 ± 0.02	36.64 ± 0.65	3.93 ± 0.91	15.13 ± 2.24	0.260	0.055	0.462	4.266	1804
2e	17.3 ± 0.93	41.67 ± 1.85	3.89 ± 0.44	25.07 ± 2.95	0.155	−0.556	0.155	3.328	1796
2f	17.3 ± 1.75	47.04 ± 0.98	12.95 ± 3.74	22.21 ± 4.38	0.583	−0.474	0.184	3.485	2141
2g	17.3 ± 1.06	27.02 ± 1.13	4.89 ± 1.29	9.31 ± 0.85	0.525	−0.220	0.952	5.157	2263
2h	23.0 ± 0.44	49.82 ± 0.17	5.21 ± 0.86	33.61 ± 7.87	0.155	−0.362	0.928	5.040	1800
2i	34.7 ± 2.47	72.25 ± 1.85	6.02 ± 0.56	24.21 ± 6.41	0.249	−0.050	0.047	3.013	1691
2j	17.3 ± 0.25	44.08 ± 1.23	10.17 ± 1.79	31.57 ± 4.71	0.321	0.270	0.330	4.165	1684
2k	17.3 ± 1.40	64.28 ± 0.61	4.31 ± 1.49	37.65 ± 4.73	0.115	−0.284	1.925	7.597	2275
2l	61.82 ± 1.54	88.54 ± 0.93	39.06 ± 7.37	36.16 ± 4.01	1.1	−0.150	0.378	3.849	1605
2m	89.36 ± 0.41	130.73 ± 3.47	59.44 ± 12.46	44.68 ± 13.23	1.33	−2.387	0.168	2.020	25
2n	52.57 ± 52.27	118.72 ± 1.70	50.52 ± 13.11	68.22 ± 22.43	0.74	−2.462	0.174	2.054	25
2o	120.94 ± 4.21	147.04 ± 3.30	111.71 ± 19.33	57.21 ± 14.71	1.95	−1.289	−0.313	1.033	136
2r	78.41 ± 1.06	95.93 ± 1.17	75.63 ± 14.08	50.27 ± 11.28	1.50	−0.217	−0.506	1.244	1402
2s	72.43 ± 1.92	73.96 ± 0.28	38.31 ± 3.67	29.67 ± 3.02	1.29	−0.027	0.525	4.347	1600
2t	66.51 ± 1.68	80.37 ± 1.10	56.41 ± 6.33	65.35 ± 13.96	0.86	−0.263	−0.424	1.417	1491
2u	106.88 ± 0.94	151.24 ± 6.17	53.51 ± 14.78	51.35 ± 3.36	1.04	−0.611	1.435	6.498	1600
3b	23.1 ± 0.01	51.56 ± 1.30	7.02 ± 3.46	25.87 ± 6.48	0.271	−0.744	0.093	3.147	1351
4b	34.7 ± 0.04	36.13 ± 1.35	9.98 ± 3.72	17.15 ± 7.92	0.582	−0.397	0.164	3.282	2184
4e	23.0 ± 1.84	49.78 ± 1.17	13.42 ± 6.19	24.86 ± 3.34	0.540	−0.542	0.156	3.392	2217
Tacrine	698.6 ± 0.12	124.73 ± 1.68	282.54 ± 55.36	55.22 ± 12.41	5.117	0.025	0.072	2.580	2828
Donepezil	32.87 ± 1.03	> 1000[b]	22.81 ± 1.25	> 1000[c]	0.014	0.082	0.617	4.426	842

[a] : The appropriate range for Log BB is between −3.0 and 1.2.
[b] : The appropriate range for Log K_{HSA} is between −1.5 and 1.5
[c] : Higher than 500 nm/s means that the compound can be adsorbed by human intestinal system.

interactions with aromatic residues in the gorge of the enzyme [24]. This result highlights possible areas for further study in a more detailed approach to the SAR. Halogenation of the para-position with bromine raised the inhibition activity for both cholinesterases (compound **2d**). In addition, fluorine- and chlorine-substituted derivatives (**2l** and **2s**) at para-position were also investigated and decreasing activity for ChEs was observed. The inhibitory effect on BChE with halogenated derivatives revealed the array Br > Cl > F. On the other hand, hydroxy and methoxy groups at the same position did not alter activity. Bromine is an atom that might participate in both hydrogen bonding with the hydrogen of an amide group [25] and halogen bonding with OH groups [26]. It was assumed the halogen and hydrogen bonds might occur on the same side, causing increased inhibition, and these two abilities might be mediated by bromine. For instance, the complex of the drug coded IDD594 with human aldose reductase was crystallized by Podjarny et al. and showed a halogen bond between bromine at the para-position of IDD594 and the OH group of threonine in the enzyme [27]. We have assumed that similar bonding might occur between **2d** and the AChE and BChE, resulting in increased activity. Electron withdrawing group NO_2 and its positions (*ortho*, *meta*, and para) were examined. Within nitro-substituted derivatives (**2m, 2n, and 2o**), the most active compound was found to be para-substituted molecules. Furthermore, C-2-substituted imidazole derivatives (**2r** and **2t**), which are without of aryl groups at the C-4 position, resulted in decreasing biological activity about 2-fold. This means that aryl groups at the C-4 position are essential for optimum biological activity.

In addition to the phenyl ring, we also tested a thienyl group (compound **2i**) for inhibition. It showed the same activity as compound **2a** did. However, it was seen that the activity of compound **2i** on BChE decreased when compared with **2a**. Bromine substituted at the C-5 position of the thienyl groups (compound **2j**) raised the inhibitory effect. The same explanation can be used for this molecule as for compound **2d**.

While reduction of the carbonyl group of **2e** decreased the inhibition constant (compound **4e**), compound **4b** did not yield any change in the inhibition of AChE but did in the inhibition of BChE. Ketoxime derivative (compound **3b**) increased inhibition from 34.65 to 23.10 nM for AChE and from 61.27 to 51.56 nM for BChE. Thus, we have seen that replacement of the carbonyl group with its reduced alcohol form or its oxime form altered biological activity slightly.

The selectivity of the synthesized molecules was also analyzed and, according to K_i values, its AChE/BChE ratio was between 0.10 and 1.95 (Table 1). The selectivity of donepezil was 0.014. Imidazole derivatives have inhibitor potency on AChE and BChE with nanomolar concentrations although donepezil, an important clinically used drug, inhibited AChE by 32.87 nM and BChE by 4030 nM (Table 1). Despite the fact that BChE activity is lower than that of AChE in the normal brain, the BChE/AChE ratio is greatly increased in AD, which suggests that inhibition of BChE may become more important as AD progresses. This raises the hypothesis that inhibitory action on both ChEs leads to improved therapeutic benefits [5,6].

Water solubility of drug candidates are important. Hence, we desired to determine the solubility data of some synthesized compounds in water using HPLC (for technical details see SI). With this experiment, we have obtained data shown in Table 2.

2.3. Toxicity of the compound 2c on different cell lines

To test the toxicity of the newly synthesized molecules, compound **2c** which was chosen due to its being more soluble in cell medium, was incubated in WS1 (skin fibroblast) and SH-SY5Y (Neuroblastoma) cell lines. The toxicity value of **2c** on the WS1 cell line was 1790 μM. This indicated that our skeleton might be safe for non-cancerous cells. In addition, toxicity on the SH-SY5Y cell line was 950 μM (Fig. 2).

Table 2
Water solubility data of some compounds.

Compounds	2c	2e	2f	4e
Water solubility (mg/mL)	1.43	0.68	0.72	44.34

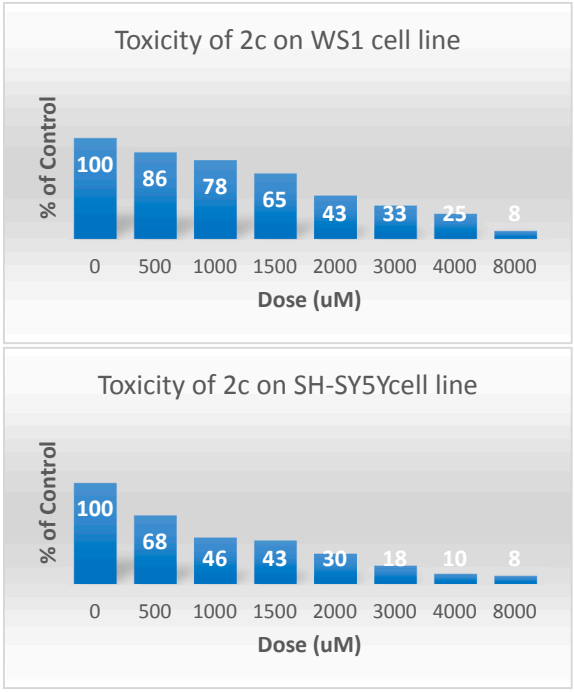

Fig. 2. Toxicity of **2c** on WS1 and on SH-SY5Y cell lines.

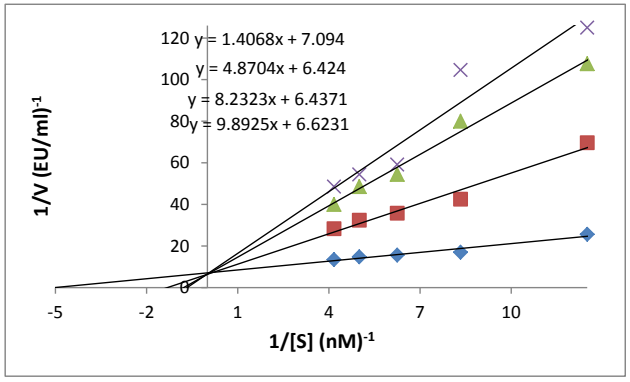

Fig. 3. Lineweaver-Burk plot of AChE for **2a**.

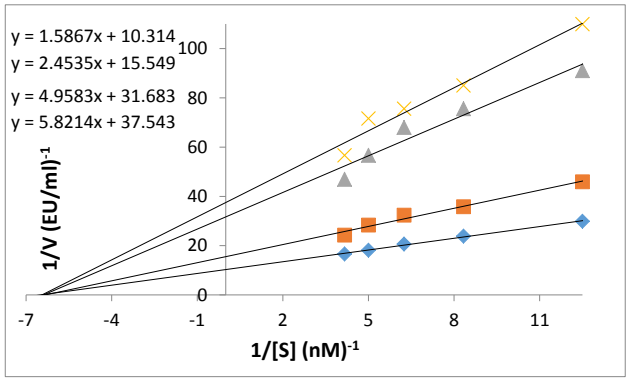

Fig. 4. Lineweaver-Burk plot of AChE for **3b**.

2.4. Kinetic studies of synthesized molecules

To get an insight into the mechanism of ChEs inhibition, all imidazole derivatives were subjected to an enzyme kinetic study (two examples of them was shown in Figs. 3–4). Lineweaver-Burk reciprocal plots showed that all tested compounds are competitive inhibitors of ChEs, except for compounds **3b** and **4e,** which showed noncompetitive inhibition on AChE (for kinetic graphics, see SI). Kinetic constants (K_i) calculated from the Lineweaver-Burk plots were between 3.89 and 111.71 nm for AChE, and between 9.31 and 68.22 nm for BChE (Table 1).

2.5. Computational studies

Potential inhibitory molecules should pass biological barriers such as the blood-brain barrier, should not bind to serum albumin, and should traverse the gut membrane. To reveal theoretically these vital parameters of the synthesized compounds, we utilized Schrödinger (qikprop) software [28]. Log BB (blood brain), Log K_{HSA} (human serum albumin binding), cLog P (lipophilicity), and Caco-2 permeability (predicted human intestinal permeability) were calculated. The predicted parameters of imidazole molecules (except for **2k,** which has two identical pyrene rings) are in good agreement with ranges, which are reported by the software (see Table 1 footnotes). Thus, the imidazole analogues are predicted to penetrate the blood brain barrier. Furthermore, Caco-2 permeability predicted that all synthesized molecules could be given orally, except for **2m, 2n,** and **2o** (nitro derivatives). Log K_{HSA} was calculated to assess the binding of imidazoles to plasma proteins such as human serum albumin, lipoprotein, and glycoprotein, because binding greatly reduces the quantity of the drug in general blood circulation. Calculated values were between −0.137 and 1.435 for Log K_{HSA}. In addition, calculations showed that all synthesized molecules except for **2k** are compliant with this parameter, indicating that imidazole derivatives are likely to circulate freely within the blood stream and access the target site (Table 1). cLog P is a popular descriptor to describe the lipophilicity of molecules. The obtained cLog P values suggested that the molecule might pass the blood-brain barrier. cLog P values for imidazoles are within the accepted range (range is reported by software and was given in Table 1), except for **2k**.

Docking studies were done using the program Autodock with the AChE X-ray crystal structure with PDB code 1B41. For the docking process, some of synthesized molecules (**2a–2k, and 4b)** were optimized using density functional theory (DFT) through the DFT/B3LYP-6-311G (d, p) method (see Table S2 in SI) [31]. The AChE active site consists of an aromatic gorge, catalytic triad (CT), peripheral anionic site (PAS), omega loop (OL), oxyanion hole (OH), anionic subsite (AS), and acyl binding pocket (ABP) [29,30]. CT side consists of Ser203, His447, and Glu334 while OH side includes Gly120, Ala204, and Gly121. One of the important side of this protein is PAS and its residues are Trp286, Tyr124, Asp74, Ser125, Tyr341, and Tyr337. Another important side of this protein is AS which includes Gly448, Glu202, Ile451, Tyr133, and Trp86.

The docking study of compound **2e** (inhibition constant 17.3 nM) was discussed in detail to observe binding to the enzyme (Fig. 5). The ligand interacted with Tyr341, Tyr124, and Tyr337 by π-sigma, hydrogen bond, and π-π interactions, respectively which are PAS side of the enzyme. On the other hand, two important interactions were observed between ligand-Glu202 (Van der Waals interaction) and ligand-Trp86 (π-sigma interaction), which form the AS active site. In addition, Gly120, important residue in the OH side, shown amide-π interaction and Van der Waals with benzene ring and its OMe group (for overlay of the other ligands see Figs. S1 and S4 in SI). In summary, it is noteworthy to say that the selected ligands interacted with important amino acid residues in the PAS, AS, and OH active sites of hAChE. These pivotal interactions might be responsible for the nanomolar activity.

3. Conclusions

To sum up, the assayed compounds are simple, low cost structures compared with the molecules in the literature. Enzyme kinetic studies presented the mechanism for inhibition of all compounds. Most of the compounds showed competitive inhibition on ChEs and two of them

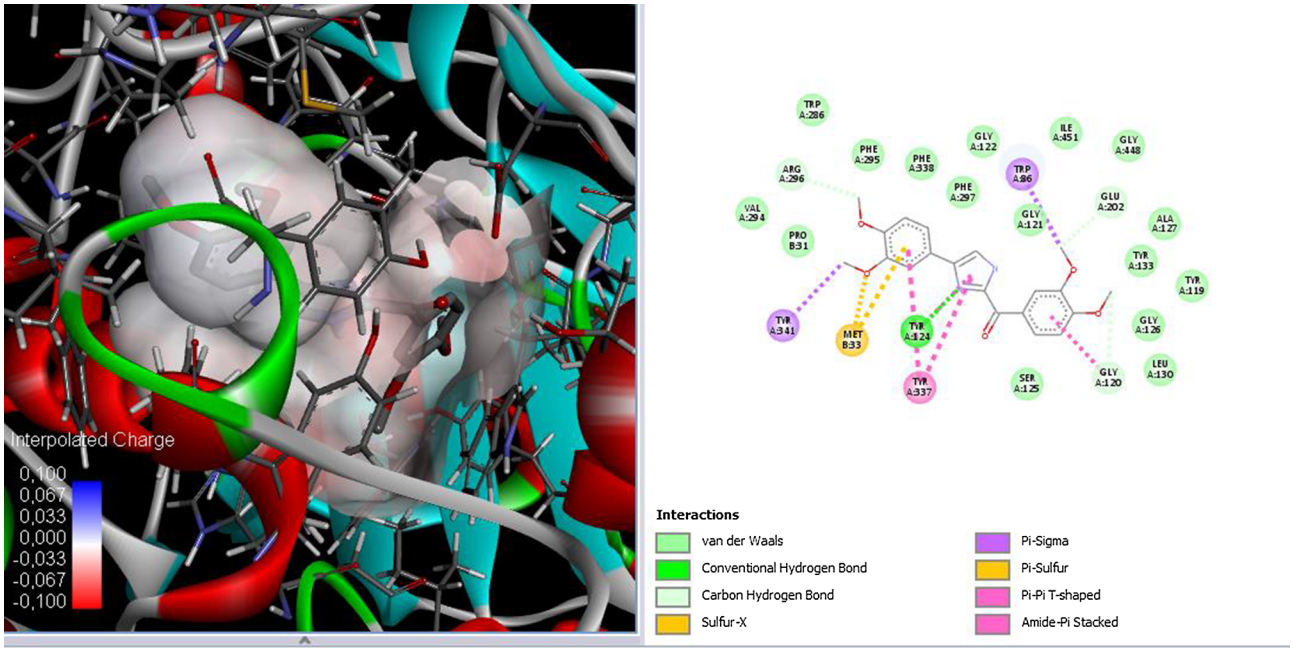

Fig. 5. Demonstration of docking study of **2e**: Noncovalent interactions between compound **2e** and some residues in hAChE (PDB code: 1B41).

showed noncompetitive inhibition on AChE. The toxicity of one compound on the WS1 and SH-SY5Y cell lines was 1790 and 950 μM, respectively. Selectivity (AChE/BChE) was between 0.10 and 1.95. ADME predictions showed some biologically important barriers such as the BBB, serum albumin, and intestinal membrane could be passed by the synthesized structures. The docking process showed that the ligand could bind to the important regions of the hAChE active side, the PAS, AS, and OH which might be a key area for further investigation. Docking scores revealed there is a common skeleton responsible for the nanomolar activity. With this information, functionalization of the skeleton might be progressed for further pre-clinical trials without losing the biological responses in ChEs inhibition. In this study, we report a previously unknown imidazole core is a potent inhibitor for ChEs with nanomolar activity. Further experiments using different functional groups and biological tests are under way.

4. Experimental section

4.1. General information for chemistry

^{1}H- and ^{13}C NMR spectra were recorded on Varian NMR-400 MHz. ^{1}H chemical shifts were referenced to internal standard TMS (δ 0.00 ppm) or (solvent d_6-DMSO). ^{13}C NMR spectra was referenced to the solvent (d_6-DMSO) peak at **33** ppm. TLC was carried out on Kieselgel 60 mesh. FT-IR spectra was recorded by Thermo Scientific, Nicoleti S10 FT-IR Spectrometer. HRMS data was recorded by Thermo Scientific, TSQ-Quantum Access with electron spray ionization technique (ESI) at positive ion detection.

4.2. General procedure for 2a–o, s, u

The commercially available acetyl substituted aromatic compounds (1 mmol) and 2.5 mmol SeO_2 were added into 4 mL 1,4-Dioxane. The reaction flask was heated at reflux temperature of solvent overnight and completion of the reaction was controlled with TLC method. Then after filtration of Se^0 particules, solution of 5 mmol ammonium acetate in ethanol was poured into the former reaction flask at room temperature. Final mixture was stirred for 1 h at room temperature. The obtained solid molecules were filtered, washed three times with water (30 mL) and dried *in vacuo* over P_2O_5.

4.3. General procedure for 2r and 2t

The imidazole (1 mmol) was dissolved in (10 mL) pyridine. Then 3 mmol triethylamine was added to the solution. The mixture was cooled with ice-water medium and stirred for 30 min. Aroyl chloride (1.5 mmol) solution which was prepared in 3.5 mL pyridine, was added to the imidazole solution as dropwise. After the reaction was stirred 30 min, 5 M 20 mL NaOH solution was added and final mixture was refluxed for 1 h. After reaction completed judged by TLC, acidic work-up was progressed. Organic phase was collected with EtOAc. EtOAc phases were evaporated and crude product was purified by column chromatography (1:5, EtOAc:*n*-hexane).

4.4. General procedure for 4b and 4e

The obtained imidazole derivatives (1 mmol) were dissolved in methanol and $NaBH_4$ (2 mmol) was added in the solution at room temperature. The solution was stirred for 2 h and the reaction completion was controlled by TLC. The mixture was recrystallized with water. And the obtained solid compound was dried with P_2O_5 at overnight.

4.5. Synthetic procedure for 3b

The synthesized compound **2b** (1 mmol) was dissolved in *n*-propanol (5 mL). 2 mmol $NH_2OH.HCl$ and TEA (2 mmol) was added into the solution. Then reaction mixture was refluxed overnight and controlled using TLC plate. After the starting compounds was disappeared on the TLC, reaction solution was cooled to room temprature. The solution was extracted with ethyl acetate (3 × 20 mL) and water. Organic layers were dried by $MgSO_4$ and evaporated.

4.5.1. Phenyl(4-phenyl-1H-imidazol-2-yl)methanone[1] (2a)

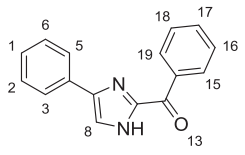

Light yellow solid, M.p: 190 °C, yield: 68.5%. FTIR (ATR) cm^{-1}:3647, 3269, 3092, 3061, 2980, 2888, 1669, 1615, 1597, 1570, 1020, 957, 935, 903, 868. ^{1}H NMR (400 MHz, DMSO) δ 8.48 (d, J = 7.11 Hz, 2H, H-19 and H-15), 8.05 (s, 1H, H-8), 7.92 (d, J = 7.11 Hz, 2H, H-3 and H-5), 7.68 (t, J = 7.50 Hz, 1H, H-17),7.60–7.58 (m, 2H, H-16 and H-18) 7.41 (t, J = 7.49 Hz, 2H, H-2 and H-6), 7.29 (t, J = 7.49 Hz, 1H, H-1). ^{13}C NMR (100 MHz, DMSO) δ 181.1, 144.7, 141.3, 136.3, 133.6, 132.5, 131.0, 129.2, 128.8, 128.1, 125.6, 120.9.

4.5.2. (4-methoxyphenyl)(4-(4-methoxyphenyl)-1H-imidazol-2-yl) methanone[2] (2b)

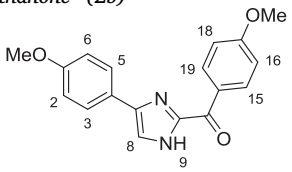

Yellow solid, M.p: 204–206 °C, yield: 87.5% FTIR (ATR) cm^{-1}: 3264, 3095, 2980, 2840, 1608, 1595, 1564, 1511, 1026, 972, 957, 903, 864. ^{1}H NMR (400 MHz, DMSO) δ 8.50–8.48 (m, AA′BB′ system, 2H, Ar-H), 7.94 (s, 1H, H-8), 7.87–7.86 (m, AA′BB′ system, 2H, Ar-H), 7.13–7.11 (m, AA′BB′ system, 2H, Ar-H), 7.00–6.68 (m, AA′BB′ system, 2H, H-2, H-6), 3.87 (s, 3H, OMe), 3.78 (s, 3H, OMe). ^{13}C NMR (100 MHz, DMSO) δ 179.1, 163.9, 159.5, 144.1, 133.5, 128.8, 127.2, 124.2, 124.1, 119.8, 114.7, 114.3, 56.1, 55.6.

4.5.3. (4-hydroxyphenyl)(4-(4-hydroxyphenyl)-1H-imidazol-2-yl) methanone[3] (2c)

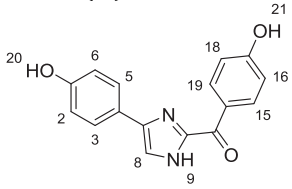

Yellow solid, M.p: 298–305 °C, yield: 56% FTIR (ATR) cm^{-1}:3647, 3233, 2980, 2889, 1607, 1579, 1433, 1029, 963, 911, 819, 806. ^{1}H NMR (400 MHz, DMSO) δ 13.27 (bs, 2H, H-20, H-21), 8.59–8.50 (m, AA′BB′ system, 2H, Ar-H), 7.77 (s, 1H, H-8), 7.76–7.73 (m, AA′BB′ system, 2H, Ar-H), 6.92–6.78 (m, AA′BB′ system, 4H, Ar-H). ^{13}C NMR (100 MHz, DMSO) δ 179.2, 162.6, 157.1, 145.1, 143.4, 133.8, 127.7, 126.6, 125.4, 116.7, 115.8, 115.5.

4.5.4. (4-bromophenyl)(4-(4-bromophenyl)-1H-imidazol-2-yl)methanone[1] (2d)

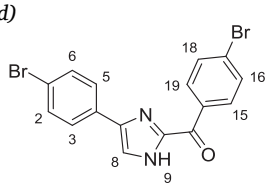

Yellow solid, M.p: 298–305 °C, yield: 56% FTIR (ATR) cm^{-1}: 3266, 3094, 1612, 1580, 1557, 1483, 1010, 902, 869, 830, 766. ^{1}H NMR (400 MHz, DMSO) δ 13.71 (bs, 1H, H-9), 8.50–8.48 (m, AA′BB′ system, 2H, Ar-H), 8.13 (bs, 1H, H-8), 7.87–7.85 (m, AA′BB′ system, 2H, Ar-H), 7.81–7.79 (m, AA′BB′ system, 2H, Ar-H), 7.60–7.59 (m, AA′BB′ system, 2H, Ar-H). ^{13}C NMR (100 MHz, DMSO) δ 180.1, 144.9, 142.3, 135.3, 133.2, 133.0, 132.0, 131.9, 127.9, 127.3, 120.6, 119.9.

4.5.5. (3,4-dimethoxyphenyl)(4-(3,4-dimethoxyphenyl)-1H-imidazol-2-yl) methanone[1] (2e)

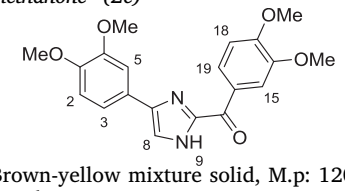

Brown-yellow mixture solid, M.p: 120–125 °C, yield: 52% FTIR (ATR) cm^{-1}: 3217, 3086, 2980, 2836, 1609, 1588, 1567, 1511, 1017, 948, 894, 856, 846. ^{1}H NMR (400 MHz, DMSO) δ 8.35 (d, J = 8.25 Hz, 1H, H-19), 7.86 (bs, 1H, H-9), 7.52 (s, 2H, H-5 and H-15), 7.52 (s, 1H, H-8), 7.12 (d, J = 8.25 Hz, 1H, H-3), 6.97 (d, J = 8.25 Hz, 1H, H-2), 3.86 (s, 3H, OMe), 3.85 (s, 3H, OMe), 3.81 (s, 3H, OMe), 3.75 (s, 3H, OMe).^{13}C NMR (100 MHz, DMSO) δ 179.1, 153.5, 149.4, 148.7, 148.5, 145.4, 128.9, 125.9, 117.9, 113.7, 112.4, 111.2, 109.1, 56.1, 55.9, 55.8, 55.7.

4.5.6. (2,6-dimethoxyphenyl)(4-(2,6-dimethoxyphenyl)-1H-imidazol-2-yl) methanone (2f)

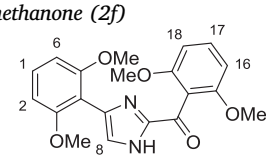

Light yellow solid, M.p, 239–241 °C, yield %30, FTIR (ATR) cm^{-1}: 3426, 3096, 3006, 2980, 2951, 1641, 1592, 1486, 1472, 1431, 950, 937, 899. ^{1}H NMR (400 MHz, $CDCI_3$) δ 11.64 (bs, 1H, H-9), 7.93 (s, 1H, H-8), 7.34 (t, $J_{17,18}$ = 8.43 Hz, 1H, H-17), 7.26 (t, $J_{1,6}$ = 8.43 Hz, 1H, H-1), 6.69 (d, $J_{18,17}$ = 8.43 Hz, 2H, H-18, H-16), 6.63 (d, $J_{6,1}$ = 8.43 Hz, 2H, H-6 and H-2), 3.97 (s, 6H, OMe) 3.75 (s, 6H, OMe).^{13}C NMR (100 MHz, $CDCI_3$) δ 184.6, 157.9, 157.5, 143.9, 134.3, 131.2, 129.4, 129.2, 117.0, 106.4, 104.4, 104.2, 56.02, 56.01. HRMS (ES) [M + H]; m/z $C_{20}H_{20}N_2O_5$:368, 1372; Found: 368, 1389.

4.5.7. naphthalen-1-yl(4-(naphthalen-1-yl)-1H-imidazol-2-yl)methanone (2 g)

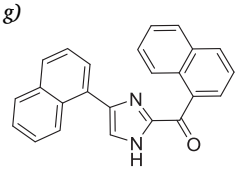

Yellow solid, M.p: 105–107 °C, yield: 61% ^{1}H NMR (400 MHz, DMSO) δ 14.0 (s, 1H, N—H), 8.60 (d, J = 8.35 Hz, 1H, Ar-H), 8.34–8.26 (m, 2H, Ar-H), 8.17 (d, J = 8.21 Hz, 1H, Ar-H), 8.07–8.05 (m, 2H, Ar-H), 7.95–7.88 (m, 2H, Ar-H), 7.75 (d, J = 6.86 Hz, 1H, Ar-H), 7.69–7.62 (m, 4H, Ar-H), 7.53–7.45 (m, 2H, Ar-H).^{13}C NMR (100 MHz, DMSO) δ 184.8, 145.3, 142.8, 134.1, 133.5, 133.2, 131.8, 130.9, 130.4, 130.2, 128.5, 128.2, 127.8, 127.3, 126.6, 126.3, 126.2, 125.9, 125.8, 125.4, 125.2, 124.6, 121.7. HRMS (ESI) [M + H] $C_{24}H_{17}N_2O$: 349, 1341; Found $(M+H)^+$: 349.1344.

4.5.8. (Naphthalen-2-yl(4-(naphthalen-2-yl)-1H-imidazol-2-yl) methanone[3] (2h)

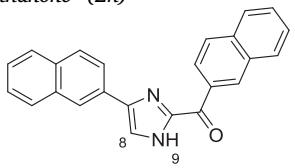

Light brown solid, M.p: 215–220 °C, yield: 72% FTIR (ATR) cm^{-1}: 3275, 3056, 1668, 1631, 1607, 1479, 1463, 1071, 1017, 961, 950, 924,

821. ^{1}H NMR (400 MHz, DMSO) δ 13.77 (s, 1H, H-9), 9.45 (s, 1H, H-8), 8.48 (bs, 1H, Ar-H), 8.26–8.24 (m, 1H, Ar-H), 8.15–8.09 (m, 2H, Ar-H), 8.03 (d, J = 8.03 Hz, 1H, Ar-H), 7.98–7.97 (m, 2H, Ar-H), 7.90 (d, J = 8.46, 1H, Ar-H), 7.70–7.65 (m, 3H, Ar-H), 7.51–7.46 (m, 3H, Ar-H). ^{13}C NMR (100 MHz, DMSO) δ 181.1, 145.5, 143.4, 135.4, 133.7, 133.5, 132.8, 132.4, 131.6, 130.5, 129.2, 128.7, 128.4, 128.3, 128.1, 127.3, 126.8, 126.3, 126.1, 124.3, 123.3, 119.7.

4.5.9. thiophen-2-yl(4-(thiophen-2-yl)-1H-imidazol-2-yl)methanone[3] (2i)

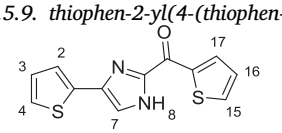

Orange solid, M.p: 195–200 °C, yield: 55% FTIR (ATR) cm^{-1}: 3235, 3092, 1644, 1594, 1506, 1473, 1051, 997, 915, 889, 870. ^{1}H NMR (400 MHz, DMSO) δ 13.67 (bs, 1H, H-8), 8.66 (dd, $J_{17,16}$ = 3.84 Hz, $J_{17,15}$ = 1.09 Hz, 1H, H-17), 8.10 (dd, $J_{2,3}$ = 4.47 Hz, $J_{2,4}$ = 1.07 Hz, 1H, H-2), 7.92 (s, 1H, H-7), 7.46 (dd, $J_{4,3}$ = 3.54 Hz, $J_{4,2}$ = 1.07 Hz, 1H, H-4), 7.45 (dd, $J_{15,16}$ = 4.98 Hz, $J_{15,17}$ = 1.09 Hz, 1H, H-15), 7.32 (dd, $J_{16,15}$ = 4.98 Hz, $J_{16,17}$ = 3.84 Hz, 1H, H-16), 7.09 (dd, $J_{3,2}$ = 4.47 Hz, $J_{3,5}$ = 3.54 Hz, 1H, H-3). ^{13}C NMR (100 MHz, DMSO) δ 173.0, 144.0, 141.1, 138.7, 137.6, 136.9, 136.6, 129.0, 128.3, 125.0, 123.4, 118.5.

4.5.10. (5-bromothiophen-2-yl)(4-(5-bromothiophen-2-yl)-1H-imidazol-2-yl)methanone (2j)

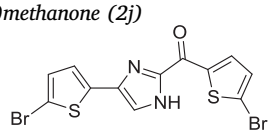

Brown solid, M.p: 170–171 °C, yield: 92% ^{1}H NMR (400 MHz, DMSO) δ 8.25 (bs, 1H, Ar-H), 7.93 (bs, 1H, Ar-H), 7.42 (d, J = 4.05 Hz, 1H, Ar-H), 7.30 (bs, 1H, Ar-H), 7.19 (d, J = 3.70 Hz, 1H, Ar-H). ^{13}C NMR (100 MHz, DMSO) δ 170.8, 143.2, 141.1, 136.2, 131.7, 131.1, 123.9, 123.7, 109.9. HRMS (ESI) [M + H] $C_{12}H_7Br_2N_2OS_2$: 416.8367; Found (M + H)$^{+}$: 416.8372.

4.5.11. Piren-1-il(4-(piren-4-il)-1H-imidazol-2-il)metanon (2k)

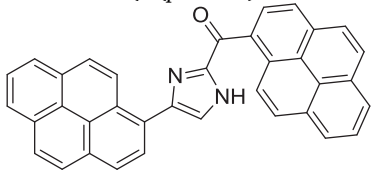

Dark brown solid, M.p: 145–149 °C, yield; 72% FTIR (ATR) cm^{-1}: 3039, 1622, 1593, 1537, 1506, 1446, 1069, 991, 959, 921, 872, 840. ^{1}H NMR (400 MHz, DMSO) δ 8.87 (d, J = 9.33 Hz, 1H, Ar-H), 8.80 (s, 1H, Ar-H), 8.63–8.61 (m, 1H, Ar-H), 8.52 (d, J = 9.33 Hz, 1H, Ar-H), 8.44 (s, 1H, Ar-H), 8.39 (d, J = 9.68 Hz, 2H, Ar-H), 8.35–8.33 (m, 1H, Ar-H), 8.32–8.31 (m, 1H, Ar-H), 8.30–8.29 (m, 1H, Ar-H), 8.28 (bs, 1H, Ar-H), 8.25–8.23 (m, 1H, Ar-H), 8.21–8.20 (m, 1H, Ar-H), 8.19–8.17 (m, 1H, Ar-H), 8.15–8.12 (m, 2H, Ar-H), 8.13–8.11 (m, 1H, Ar-H), 8.08 (bs, 1H, Ar-H), 8.03–8.01 (m, 1H, Ar-H). ^{13}C NMR (100 MHz, DMSO) δ 185.5, 146.7, 133.3, 132.1, 131.4, 131.1, 130.8, 130.7, 130.5, 129.8, 129.7 129.5, 129.3, 128.0, 127.9, 127.8, 127.7, 127.6, 127.2, 126.8, 126.5 125.7, 125.4, 125.3, 125.0, 124.8, 124.4, 124.3, 124.2, 124.0. HRMS (ESI) [M + H] $C_{36}H_{21}N_2O$: 497.1654; Found (M + H)$^{+}$: 497.1649.

4.5.12. (4-fluorophenyl)(4-(4-fluorophenyl)-1H-imidazol-2-yl)methanone (2l)

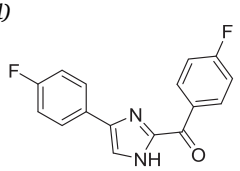

Dark yellow solid, M.p: 224–226 °C. Yield % 92. ^{1}H NMR (400 MHz, d_6-DMSO) δ = 13.6 (bs, 1H, −NH), 8.71–8.67 (m, AA′BB′ system, 2H, Ar-H), 8.06 (d, J = 2.51 Hz, 1H, Ar-H), 7.96–7.93 (m, AA′BB′ system, 2H, Ar-H), 7.44–7.39 (m, AA′BB′ system, 2H, Ar-H), 7.26–7.22 (m, AA′BB′ system, 2H, Ar-H). ^{13}C NMR (100 MHz, d_6-DMSO) δ = 179.5, 166.8, 164.3, 163.1, 160.7, 144.9, 142.5, 134.1 (d, J = 9.39 Hz), 133.5, 132.9, 130.6, 127.2 (d, J = 8.05 Hz), 127.2, 119.0, 116.0 (d, J = 6.26 Hz), 115.8 (d, J = 6.58 Hz). HRMS (ES) [M + H]; m/z $C_{16}H_{11}F_2N_2O$:285.08394; Found [M + H]: 285.08385.

4.5.13. (3-nitrophenyl)(4-(3-nitrophenyl)-1H-imidazol-2-yl)methanone (2m)

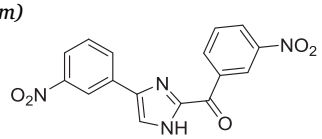

Light brown solid, M.p: 210–212 °C. Yield % 89. ^{1}H NMR (400 MHz, d_6-DMSO) δ = 13.94 (bs, 1H, −NH), 9.49–9.48 (m, 1H, Ar-H), 8.87–8.85 (m, 1H, Sr-H), 8.70–8.66 (m, 1H, Ar-H), 8.51–8.47 (m, 1H, Ar-H), 8.36–8.30 (m, 2H, Ar-H), 8.11–8.08 (m, 1H, Ar-H), 7.89–7.85 (m, 1H, Ar-H), 7.71–7.66 (m, 1H, Ar-H). ^{13}C NMR (100 MHz, d_6-DMSO) δ = 178.6, 148.8, 148.0, 144.8, 141.3, 137.1, 136.9, 135.6, 131.4, 130.7, 130.6, 127.8, 126.0, 122.2, 121.3, 119.4. HRMS (ES) [M + H]; m/z $C_{16}H_{11}N_4O_5$:339.07294; Found [M + H]: 339.07211.

4.5.14. (4-nitrophenyl)(4-(4-nitrophenyl)-1H-imidazol-2-yl)methanone (2n)

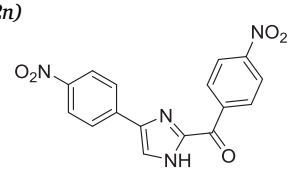

Dark Brown solid, M.p: 280–282 °C. Yield 88%. ^{1}H NMR (400 MHz, d_6-DMSO) δ = 8.71–8.68 (m, AA′BB′ system, 2H, Ar-H), 8.42 (bs, 1H, Ar-H),8.42–8.40 (m, AA′BB′ system, 2H, Ar-H), 8.28–8.26 (m, AA′BB′ system, 2H, Ar-H), 8.18–8.16 (m, AA′BB′ system, 2H, Ar-H). ^{13}C NMR (100 MHz, d_6-DMSO) δ = 180.1, 150.2, 146.6, 145.3, 141.5, 141.2, 132.4, 126.0, 124.6, 123.8. HRMS (ES) [M + H]; m/z $C_{16}H_{11}N_4O_5$:339.07294; Found [M + H]: 339.07288.

4.5.15. (2-nitrophenyl)(4-(2-nitrophenyl)-1H-imidazol-2-yl)methanone (2o)

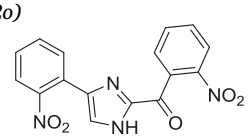

Light brown solid, M.p: 236–237 °C. Yield % 75. ^{1}H NMR (400 MHz, d_6-DMSO) δ = 13.12 (bs, 1H, −NH), 8.50 (dd, J = 0.95 Hz, J = 8.30 Hz, 1H, Ar-H), 8.26 (dd, J = 0.95 Hz, J = 8.30 Hz, 1H, Ar-H), 8.09 (dd, J = 1.43 Hz, J = 7.89 Hz, 1H, Ar-H), 7.98 (J = 1.12 Hz, J = 7.51 Hz, 1H, Ar-H), 7.90–7.86 (m, 2H, Ar-H), 7.80 (dd, J = 1.39 Hz, J = 7.48 Hz, 1H, Ar-H), 7.62–7.58 (m, 1H, Ar-H), 7.26–7.22 (m, 1H, Ar-H), ^{13}C NMR (100 MHz, d_6-DMSO) δ = 188.9, 170.0, 158.0, 148.2, 135.7, 134.3, 133.2, 132.0, 131.9, 130.7, 124.5, 124.1, 119.9. HRMS (ES) [M + H]; m/z $C_{16}H_{11}N_4O_5$:339.07294; Found [M + H]: 339.07278.

4.5.16. (1H-imidazol-5-yl)(thiophen-2-yl)methanone (2r)

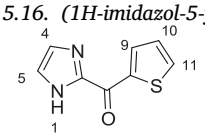

Light yellow solid, M.p: 162–164 °C. Yield 75%. ^{1}H NMR (400 MHz, $CDCl_3$) δ = 8.72 (dd, $J_{11,9}$ = 1.26 Hz, $J_{11,10}$ = 3.86 Hz, 1H, H-11), 7.77 (dd, $J_{9,11}$ = 1.26 Hz, $J_{9,10}$ = 4.95 Hz, 1H, H-9,), 7.35 (bs, 2H, H-4,5), 7.21 (dd, $J_{10,11}$ = 3.86 Hz, $J_{10,9}$ = 4.95 Hz, 1H, H-10). ^{13}C NMR

(100 MHz, $CDCl_3$) δ = 174.1, 144.6, 140.3, 137.0, 135.8, 128.3. HRMS (ES) [M + H]; *m/z* $C_8H_7N_2OS$:179.02791; Found [M + H]: 179.02701.

4.5.17. (4-chlorophenyl)(4-(4-chlorophenyl)-1H-imidazol-2-yl)methanone (2 s)

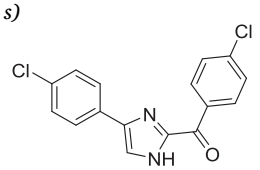

Light brown solid, M.p: 189–191 °C. Yield 90%. ^{1}H NMR (400 MHz, d_6-DMSO) δ = 13.72 (bs, 1H, −NH), 8.60–8.56 (m, AA′BB′ system, 2H, Ar-H), 8.13 (d, *J* = 2.53 Hz, 1H, Ar-H), 7.94–7.91 (m, AA′BB′ system, 2H, Ar-H), 7.67–7.64 (m, AA′BB′ system, 2H, Ar-H), 7.49–7.44 (m, AA′BB′ system, 2H, Ar-H). ^{13}C NMR (100 MHz, d_6-DMSO) δ = 179.8, 144.9, 142.2, 138.6, 134.9, 132.9, 132.8, 132.1, 132.0, 129.1, 128.9, 127.0, 119.8. HRMS (ES) [M + H]; *m/z* $C_{16}H_{11}Cl_2N_2O$:317.02484; Found [M + H]: 317.02446.

4.5.18. (1H-imidazol-5-yl)(phenyl)methanone (2t)

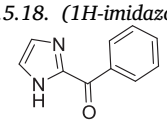

Brown Viscous liquid, Yield 65%. ^{1}H NMR (400 MHz, $CDCl_3$) δ = 11.33 (bs, 1H, −NH), 8.59–8.56 (m, 2H, Ar-H), 7.63–7.59 (m, 1H, Ar-H), 7.53–7.49 (m, 2H, Ar-H), 7.41 (bs, 1H, Ar-H), 7.27 (bs, 1H, Ar-H). ^{13}C NMR (100 MHz, $CDCl_3$) δ = 182.2, 145.2, 135.6, 133.4, 131.8, 131.0, 128.3, 120.3. HRMS (ES) [M + H]; *m/z* $C_{10}H_9N_2O$:173.07149; Found [M + H]: 173.07149.

4.5.19. [1,1′-biphenyl]-4-yl(4-([1,1′-biphenyl]-4-yl)-1H-imidazol-2-yl) methanone (2u)

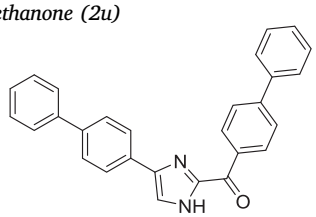

Brown solid, M.p: 284–286 °C. Yield 86%. ^{1}H NMR (400 MHz, d_6-DMSO) δ = 8.69–8.67 (m, AA′BB′ system, 2H, Ar-H), 8.10 (bs, 1H, Ar-H), 8.04–8.02 (m, AA′BB′ system, 2H, Ar-H), 7.92–7.90 (m, AA′BB′ system, 2H, Ar-H), 7.80–7.79 (m, AA′BB′ system, 2H, Ar-H), 7.76–7.70 (m, 4H, Ar-H), 7.53–7.43 (m, 5H, Ar-H), 7.37–7.34 (m, 1H, Ar-H). ^{13}C NMR (100 MHz, d_6-DMSO) δ = 180.5, 144.9, 135.2, 131.9, 129.6, 139.4, 128.9, 127.9, 127.5, 127.4, 127.0, 126.9, 126.0. HRMS (ES) [M + H]; *m/z* $C_{28}H_{21}N_2O$:401.16539; Found [M + H]: 401.16531.

4.5.20. (Z-E)-(4-methoxyphenyl)(4-(4-methoxyphenyl)-1H-imidazol-2-yl) methanone oxime (3b)

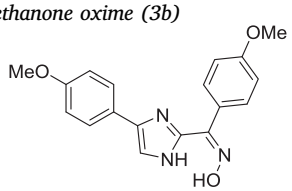

Light brown viscous, yield: 89.2% ^{1}H NMR (400 MHz, DMSO) δ 12.29 (s, 1H, N−H), 11.30 (s, 1H, O−H), 7.73–7.65 (m, 1H, Ar-H), 7.63–7.60 (m, 2H, Ar-H), 7.55–7.53 (m, 1H, Ar-H), 7.51–7.47 (m, 1H, Ar-H), 6.99–6.94 (m, 2H, Ar-H), 6.92–6.90 (m, 1H, Ar-H), 6.87–6.85 (m, 1H, Ar-H), 3.80–3.78 (m, 3H, OMe), 3.76–3.72 (m, 3H, OMe). ^{13}C NMR (100 MHz, DMSO) δ 160.1, 159.8, 158.3, 147.9, 143.8, 141.2, 132.0, 127.7, 126.0, 123.9, 114.6, 114.4, 114.2, 113.6, 113.5, 113.2, 55.6, 55.5. HRMS (ESI) [M + H] $C_{18}H_{18}N_3O_3$: 324.1348; Found $(M+H)^+$: 324.1350.

4.5.21. (4-methoxyphenyl)(4-(4-methoxyphenyl)-1H-imidazol-2-yl) methanol (4b)

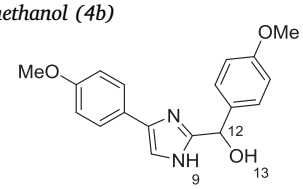

Light brown solid, M.p: 180–181 °C, yield: 87% ^{1}H NMR (400 MHz, DMSO) δ 11.91 (s, 1H, H-9), 7.63 (d, *J* = 8.76 Hz, 2H, Ar-H), 7.35 (d, *J* = 8.67 Hz, 3H, Ar-H), 6.89–6.85 (m, 4H, Ar-H), 6.10 (d, $J_{13,12}$ = 3.96, 1H, H-13), 5.70 (d, $J_{12,13}$ = 3.96, 1H, H-12), 3.72 (s, 3H, OMe), 3.70 (s, 3H, OMe). ^{13}C NMR (100 MHz, DMSO) δ 158.8, 158.1, 135.7, 128.1, 125.9, 114.2, 113.8, 69.7, 55.5, 55.4. HRMS (ESI) [M + H] $C_{18}H_{19}N_2O_3$: 311.1396; Found $(M+H)^+$: 311.1397.

4.5.22. (3,4-dimethoxyphenyl)(4-(3,4-dimethoxyphenyl)-1H-imidazol-2-yl)methanol (4e)

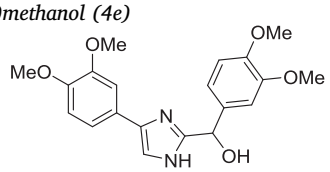

Light pink solid, M.p: 210–211 °C, yield: 75% FTIR (ATR) cm^{-1}: 3288, 3113, 3008, 2954, 2904, 1591, 1532, 1511, 1451, 1320, 944, 871, 854. ^{1}H NMR (400 MHz, d_6-DMSO) δ 11.96 (bs, 1H, N−H), 7.35 (bs, 1H, Ar-H), 7.31 (d, *J* = 1.96 Hz, 1H, Ar-H), 7.24 (dd, *J* = 1.96, *J* = 8.29 Hz, 1H, Ar-H), 7.14 (d, *J* = 1.58 Hz, 1H, Ar-H), 6.92–6.88 (m, 3H, Ar-H), 6.13 (d, *J* = 3.39 Hz, 1H, OH), 5.70 (d, *J* = 3.39 Hz, 1H, CH) 3.78 (s, 3H, OMe), 3.75(s, 3H, OMe), 3.73 (s, 3H, OMe), 3.71 (s, 3H, OMe). ^{13}C NMR (100 MHz, d_6-DMSO) δ 151.2, 149.2, 148.9, 148.4, 147.7, 136.1, 119.0, 116.8, 112.4, 111.8, 110.7, 108.6, 69.9, 56.0, 55.9, 55.8, 55.7. HRMS (ESI) [M + H] $C_{20}H_{23}N_3O_5$: 371. 1607; found $(M+H)^+$: 371.1600.

4.6. hAChE and hBChE activity determination and inhibition studies

In bioactivity studies, colorimetric Ellman method was slightly modified and enzyme inhibition was examined [4]. Acetylthiocholine iodide (AChI) and butyrylthiocholine iodide (BChI) were used as substrates for the reaction. 5,5′-Dithio-bis(2-nitro-benzoic)acid (DTNB) was used for the measurement of the AChE and BChE activities. In vitro enzyme activity studies was performed using recombinant human AChE and human serum BChE enzymes. Activity process was utilized as followed; To deionized water, 1.0 mL of Tris/HCl buffer (1.0 M, pH 8.0), and 10 mL of sample solution at different concentrations were added. And then 50 mL AChE or BChE solution were mixed and the final solution was incubated for 10 min at 25 °C. After incubation, 50 mL of DTNB (0.5 mM) was added. The reaction was allowed to be initiated upon addition of 50 mL of AChI or BChI. The hydrolysis of these substrates was monitored spectrophotometrically by the formation of the yellow 5-thio-2-nitrobenzoate anion, as a result of the reaction of DTNB with thiocholine, which released by enzymatic hydrolysis of AChI or BChI, with absorption maximum at 412 nm. IC_{50} values were obtained from activity (%) versus compounds plots. On the other hand, Ki values were obtained from Lineweaver-Burk graph. All the experiments were

performed at least three times (N = 3).

4.7. Docking studies

For some of synthesized compounds, the structure-based docking method was applied to determine the binding and interaction points of the enzymes in the active regions and protein-ligand interaction analysis was carried out on the crystal structures, coded 1B41. Autodock program was used and the Protein Preparation Wizard protocol was followed for docking studies. The compounds to be analyzed were optimized by DFT calculation (DFT/B3LYP-6-311G (d,p)) with Gaussian 09. When docking process was applied, grid box was determined. Grid box was used to construct a grid with single precision (SP) and enzyme interaction energies (docking scores) were recorded.

5. Cytotoxicity assay with MTT

Preparation of the MTT solution: For the method to be used in the study, the 5 mg MTT dye contained in the package will be vortexed after dissolving in 1 mL of sterile phosphate buffer (PBS) and the insoluble parts will be centrifuged and the supernatant will be taken to a sterile ependorum. The MTT solution that is sensitive to light will be stored in the dark at +4 °C until use. Prior to the application of the MTT protocol, the cells must be prepared for this assay.

Preparation of Cell Cultures in 96-well plates: The cell lines (WS1 and SH-SY5Y) were firstly counted and planted in cell plates (96-well plates at 8×10^3 cells/well density). Sterile water or PBS was added to the outermost of the wells to prevent evaporation. Other fields was used for the experiment. Cells were regularly and evenly distributed between the wells and whether they are healthy or not was examined under microscope. The cells shown in the wells was incubated for 24 h.

Addition of synthesized compound (**2c**) to cells: After 24 h of incubation, the cells were re-incubated with the final concentration of **2c** (1, 500, 1000, 1500, 2000, 3000, 4000, 8000 μM) for 96 h.

Making the MTT experiment: After 96 h, the medium was pipetted in the wells removed from the incubator. 200 mL PBS was added to the wells to thoroughly clean the wells. Then addition of 100 μL of fresh medium to each well and 10 μL of MTT solution were progressed and the final solution was incubated in the incubator for 4 h. At the end of 4 h, 100 μL of sodium dodecyl sulfate (SDS) was added to the wells and incubated for 12 h at 37 °C in a CO_2 incubator to dissolve formazone crystals formed with MTT. The culture plate was placed on the microplate reader and absorbance values was read at 570 nm. This value was accepted as 100% by taking the average of the absorbance values obtained from the control cultures with no added substances. The absorbance values obtained from the cultures containing the synthesis compounds was proportioned to the control absorbance value and the viability rates of the cells was expressed as%. These experiments were carried out with at least 4 replicates.

Author contributions

The manuscript was written through contributions of all authors. All authors have given approval to the final version of the manuscript.

Notes

The authors declare no competing financial interest.

Acknowledgement

This study was partly funded by Scientific and Technologic Research Agency of Turkey (TÜBİTAK) (grant numbers: 115Z112, 115Z894)

Appendix A. Supplementary material

Supplementary data to this article can be found online at https://doi.org/10.1016/j.bioorg.2019.01.044.

References

[1] M. Burkart, R. Heun, O. Benkert, Serial position effects in dementia of the Alzheimer type, Dement Geriatr. Cogn. Diso. 9 (1998) 130–136.
[2] R.J. Hargreaves, "It Ain't Over 'til It's Over"[a] The search for treatments and cures for Alzheimer's disease, ACS Med. Chem. Lett. 3 (2012) 862–866.
[3] D.S. Geldmacher, Acetylcholinesterase inhibitors for Alzheimer's disease, Aging Health 3 (2007) 483–494.
[4] S.M. Li, M.S. Xu, P.Y. Mo, Progress, in mechanisms of acetylcholinesterase inhibitors and memantine for the treatment of Alzheimer's disease, Neuroimmunol. Neuroinflamm. 2 (2015) 274–280.
[5] T. Arendt, M.K. Bruckner, M. Lange, V. Bigl, Changes in acetylcholinesterase and butyrylcholinesterase in Alzheimers-disease resemble embryonic-development—A study of molecular-forms, Neurochem. Int. 21 (1992) 381–396.
[6] R.M. Lane, S.G. Potkin, A. Enz, Targeting acetylcholinesterase and butyrylcholinesterase in dementia, Int. J. Neuropsychopharmacol. 9 (2006) 101–124.
[7] B. Özgeriş, S. Göksu, K.L. Polat, İ. Gülçin, R.E. Salmas, S. Durdagi, F. Tümer, C.T. Supuran, Acetylcholinesterase and carbonic anhydrase inhibitory properties of novel urea and sulfamide derivatives incorporating dopaminergic 2-aminotetralin scaffolds, Bioorg. Med. Chem. 4 (2016) 2318–2329.
[8] S.C. Samuels, K.L. Davis, A risk-benefit assessment of tacrine in the treatment of Alzheimer's disease, Drug Saf. 16 (1997) 66–77.
[9] Y. Kawakami, A. Inoue, T. Kawai, M. Wakita, H. Sugimoto, A. Hopfinger, The rationale for E2020 as a potent acetylcholinesterase inhibitor, Bioorg. Med. Chem. 4 (1996) 1429–1446.
[10] J. Seibert, F. Tracik, K. Articus, S. Spittler, Effectiveness and tolerability of transdermal rivastigmine in the treatment of Alzheimer's disease in daily practice, Neuropsychiatr. Dis. Treat. 8 (2012) 141–147.
[11] H.M. Greenblatt, G. Kryger, T. Lewis, I. Silman, J.L. Sussman, Structure of acetylcholinesterase complexed with (-)-galanthamine at 2.3 A resolution, FEBS Lett. 463 (1999) 321–326.
[12] O.M. B.-Aguilera, A. Samadi, M. Chioua, K. Nikolic, S. Filipic, D. Agbaba, E. Soriano, L.R. Andres, M.I. Franco, S. Alcaro, R.R. Ramsay, F. Ortuso, M. Yanez, M.J. Contelles, *N*-Methyl-*N*-((1-methyl-5-(3-(1-(2-methylbenzyl)piperidin-4-yl)propoxy)-1*H*-indol-2-yl)methyl)prop-2-yn-1-amine, a new cholinesterase and monoamine oxidase dual inhibitor, J. Med. Chem. 57 (2014) 10455–10463.
[13] B. Sameem, M. Saeedi, M. Mahdavi, A. Shafiee, A review on tacrine-based scaffolds as multi-target drugs (MTDLs) for Alzheimer's disease, Eur. J. Med. Chem. 128 (2017) 332–345.
[14] Z. Luo, J. Sheng, Y. Sun, C. Lu, J. Yan, A. Liu, H. Luo, L. Huang, X. Li, Synthesis and evaluation of multi-target-directed ligands against Alzheimer's disease based on the fusion of Donepezil and Ebselen, J. Med. Chem. 56 (2013) 9089–9099.
[15] J. Correa-Basurto, I.V. Alcantara, L.M. Espinoza-Fonseca, J. Trujillo-Ferrara, *p*–Aminobenzoic acid derivatives as acetylcholinesterase inhibitors, Eur. J. Med. Chem. 116 (2005) 732–735.
[16] A. Rampa, M. Bartolini, A. Bisi, F. Belluti, S. Gobbi, V. Andrisano, A. Ligresti, V. Marzo, The first dual ChE/FAAH inhibitors: new perspectives for Alzheimer's disease? ACS Med. Chem. Lett. 3 (2012) 182–186.
[17] (a) M.W. Moon, C.G. Chidester, R.F. Heier, J.K. Morris, R.J. Collins, R.R. Russell, J.W. Francis, G.P. Sage, V.H. Sethy, Cholinergic activity of acetylenic imidazoles and related compounds, J. Med. Chem. 34 (1991) 2314–2327;
(b) A.S. Gurjar, M.N. Darekar, K.Y. Yeong, L. Ooi, In silico studies, synthesis and pharmacological evaluation to explore multi-targeted approach for imidazole analogues as potential cholinesterase inhibitors with neuroprotective role for Alzheimer's disease, Bioorg. Med. Chem. 26 (2018) 1511–15222.
[18] B. Kuzu, M. Tan, Z. Ekmekci, N. Menges, A novel fluorescent sensor based on imidazole derivative for Fe3+ ions, J. Lumin. 192 (2017) 1096–1103.
[19] A. Hiremathad, K. Chand, L. Tolayan, R.S. Keri, A.R. Esteves, S.M. Cardoso, S. Chaves, M.A. Santos, Hydroxypyridinone-benzofuran hybrids with potential protective roles for Alzheimeŕs disease therapy, J. Inorg. Biochem. 179 (2018) 82–96.
[20] J. Wang, C. Wang, Z. Wu, X. Li, S. Xu, J. Liu, Q. Lan, Z. Zhu, J. Xu, Design, synthesis, biological evaluation, and docking study of 4-isochromanone hybrids bearing N-benzyl pyridinium moiety as dual binding site acetylcholinesterase inhibitors (part II), Chem. Biol. Drug. Des. 91 (2018) 756–761.
[21] H. Sugimoto, Y. Yamanishi, Y. Limura, Y. Kawakami, Curr. Med. Chem. 7 (2000) 303–339.
[22] P. Costanzo, L. Cariati, D. Desiderio, R. Sgammato, A. Lamberti, R. Arcone, R. Salerno, M. Nardi, M. Masullo, M. Oliverio, Design, synthesis, and evaluation of donepezil-like compounds as AChE and BACE–1 inhibitors, ACS Med. Chem. Lett. 7 (2016) 470–475.
[23] C.V. Andersson, N. Nina Forsgren, C. Akfur, A. Allgardsson, L. Berg, C. Engdahl, W. Ekström Qian, F. Linusson, Divergent structure-activity relationships of structurally similar acetylcholinesterase inhibitors, J. Med. Chem. 56 (2016) 7615–7624.
[24] D. Patrick, An Introduction to Medicinal Chemistry, Oxford University Press,

Oxford, 2017, pp. 650–651.
[25] A. Chandrasekaran, Current trends in X-Ray crystallography. intramolecular N−H···X (X = F, Cl, Br, I, and S) hydrogen bonding in aromatic amide derivatives – The X-Ray crystallographic investigation, D.-Wei Zhang, Z.-Ting Li, InTech Publishing, Croatia, pp. 95–112, 2011.
[26] K.D. Collins, G.W. Neilson, J.E. Enderby, Ions in water: characterizing the forces that control chemical processes and biological structure, Biophys. Chem. 128 (2007) 95–104.
[27] E.I. Howard, R. Sanishvili, R.E. Cachau, A. Mitschler, B. Chevrier, P. Barth, V. Lamour, Z.M. Van, E. Sibley, C. Bon, D. Moras, T.R. Schneider, A. Joachimiak, A. Podjarny, Ultrahigh resolution drug design I: details of interactions in human aldose reductase-inhibitor complex at 0.66 A, Protein 55 (2004) 792–804.
[28] Schrödinger Release 2017-4: Qikprop, Schrödinger, LLC, Newyork, NY, 2017, trial licence.
[29] F.D. Silva, P.A. Nogara, M.M. Braga, B.C. Piccoli, J.B.T. Rocha, Molecular docking analysis of acetylcholinesterase corroborates the protective effect of pralidoxime against chlorpyrifos-induced behavioral and neurochemical impairments in Nauphoeta cinerea, Compt. Toxycology 8 (2018) 25–33.
[30] L. Wang, I. Moraleda, I. Iriepa, A. Romera, F. Lopez-Munoz, M. Chioua, T. Inokuchi, M. Bartolini, J. Marco-Contelles, 5-Methyl-N-(8-(5,6,7,8-tetrahydroacridin-9-ylamino)octyl)-5H-indolo[2,3-b]quinolin-11-amine: a highly potent human cholinesterase inhibitor, Medchemcomm 8 (2017) 1307–1317.
[31] M.J. Frisch, et al., Gaussian 09, Revision D.01, Gaussian, Inc., Wallingford CT, 2009.